

## Examining the use of time domain reflectometry for measuring liquid water content in frozen soil

Egbert J. A. Spaans and John M. Baker

Department of Soil, Water, and Climate, University of Minnesota, St. Paul  
Agricultural Research Service, U.S. Department of Agriculture, St. Paul, Minnesota

**Abstract.** Time domain reflectometry (TDR) offers a unique opportunity to measure liquid water content  $\theta_L$  in frozen soil, since the permittivity of ice is much lower than that of water. However, calibrations of TDR derived from drying unfrozen soil, where water is replaced by air, may not apply to a freezing soil, where water is replaced by ice, since the permittivity of ice is greater than that of air. We designed a gas dilatometer to calibrate TDR for  $\theta_L$  in frozen soil. A soil sample is hermetically sealed in the gas dilatometer; subsequent soil freezing reduces total air space and hence increases pressure inside the gas dilatometer, since ice is less dense than water. The amounts of soil water frozen were computed from measured pressure change as temperature was incrementally decreased. TDR calibrations for two samples of the same soil at different total water contents had identical slopes but different intercepts, supporting our hypothesis that there exists no unique calibration of TDR for  $\theta_L$  for frozen soil, but rather a family of calibration curves, each curve corresponding to a different total water content.

### Introduction

Soil water contents affect many processes that are of interest in the environmental sciences, including transport processes in soil, infiltration, evaporation, and plant water uptake. Most of these phenomena proceed throughout the year, even when soils are frozen, because soils freeze over a range of temperatures, with liquid water present in a continuous film adsorbed to mineral and organic surfaces even at temperatures well below the freezing point. It is therefore necessary to consider soil water distribution on a year-round basis, which at higher latitudes includes substantial periods in which at least parts of soil profiles are frozen.

The measurement of water content in unfrozen soil is well documented [Gardner, 1986; Baker, 1990]. Methods include gravimetry, neutron thermalization, gamma densitometry, and more recently nuclear magnetic resonance (NMR) and time domain reflectometry (TDR). The measurement of liquid water content in frozen soil is more complicated, primarily due to the presence of the ice phase. Thus when these techniques are to be applied to frozen soil, their relative sensitivity to the different phases of water must be well understood [Nieber *et al.*, 1992].

Gravimetric sampling, the reference for water-content measurement, yields total water content  $\theta$ , which is unfrozen water content  $\theta_L$  and ice content  $\theta_i$  combined. The neutron probe counts thermalized neutrons, which result predominantly from collisions with hydrogen atoms in a volume of soil. Since fast neutrons are thermalized in the same way regardless of whether the soil water is in the liquid or solid form, the neutron probe cannot detect the difference between these two phases and thus measures  $\theta$ . Gamma densitometry is based on the attenuation of photons through their interactions with electrons of an intervening medium. The attenuation is indepen-

dent of the phase composition of the medium [Hoekstra, 1966; Goit *et al.*, 1978], so this method cannot distinguish between liquid and frozen water and measures  $\theta$  as well. NMR determination of soil water is based on the principle that hydrogen protons resonate when subjected to an oscillating magnetic field. The NMR can be tuned to hydrogen associated with either liquid water or ice [Tice *et al.*, 1982] and can therefore determine  $\theta_L$  or  $\theta_i$ . Unfortunately, there are drawbacks to widespread, routine use of NMR, including (1) it is not suitable for in situ measurements because the apparatus would disturb the soil sample and the flow of heat and water to and from the soil [Oliphant, 1985], (2) magnetic particles in the soil interfere with the measurement, (3) it cannot be automated, and (4) it is expensive.

TDR measures the travel time of an electromagnetic wave through a medium, which is a function of the permittivity  $\epsilon$  of the individual components of the medium, their volumetric fractions, and their geometric arrangement. This should permit estimation of  $\theta_L$  in frozen soil, since  $\epsilon$  of water is much higher than that of other soil constituents, including ice. Moreover, TDR is suitable for in situ measurements, is easily automated and multiplexed, and can be left unattended in the field [Baker and Allmaras, 1990; Heimovaara and Bouten, 1990]. Finally, TDR permits simultaneous measurement of  $\theta_L$  and bulk electrical conductivity, a feature enhanced by recent developments in probe design [Spaans and Baker, 1993]. These capabilities make the method attractive for solute transport research, but year-round use in areas subject to seasonal freezing is limited by uncertainties in calibrations for  $\theta_L$ .

Application of TDR in frozen soils requires knowledge of the relationship between  $\epsilon$  of the soil and  $\theta_L$ . However, existing calibrations based on drying and wetting of unfrozen soils are not necessarily applicable because during drying, water is replaced by air, whereas during freezing, water is replaced by ice, which has a slightly higher  $\epsilon$  than air. Our objectives are to demonstrate a new method to calibrate TDR for liquid water content in frozen soil and to evaluate the role of initial water content on the calibration.

Copyright 1995 by the American Geophysical Union.

Paper number 95WR02769.  
0043-1397/95/95WR-02769\$05.00

## TDR Calibration: Hypothesis

Calibrations of TDR in unfrozen soil are based on simultaneous measurements of  $\theta$  and travel time of the TDR signal through a soil at various degrees of saturation. When soils freeze, however, ice forms in situ at the expense of  $\theta_L$ . At identical liquid water contents a freezing soil should have a higher  $\varepsilon$  than a drying soil because  $\varepsilon$  for ice is 3.2 compared to 1 for air. Consequently, calibration derived in unfrozen soil should systematically overpredict  $\theta_L$  in frozen soil because it ascribes the higher value for  $\varepsilon$  to additional water rather than to the contribution from ice.

This dilemma was recognized by several scientists. *Patterson and Smith* [1981] found that replacing air with ice at constant  $\theta_L$  increased the soil  $\varepsilon$  slightly, but the increase was insignificant compared to their overall variation in  $\varepsilon$  determination. They concluded that the same calibration equation is applicable to both frozen and unfrozen soils. *Oliphant* [1985], on the other hand, found that a separate calibration equation was required for frozen soil. He proposed a dielectric mixing model which predicted  $\theta_L$  best when using an  $\varepsilon$  of 9.2 for the soil mineral phase and 67.8 for water, values quite different from those typically reported (i.e., 3 to 5 for minerals and 88 for water at 0°C). *Smith and Tice* [1988] calibrated TDR for frozen soil in small, saturated samples using NMR to determine  $\theta_L$ , and found

$$\theta_L = -1.458 \times 10^{-1} + 3.868 \times 10^{-2}\varepsilon - 8.502 \times 10^{-4}\varepsilon^2 + 9.920 \times 10^{-6}\varepsilon^3 \quad (1)$$

Since (1) is based on saturated frozen soils, it should systematically underestimate  $\theta_L$  if applied to unsaturated frozen soil, because at equal  $\theta_L$  the mix of air and ice in unsaturated soil leads to a lower  $\varepsilon$  than does ice alone.

Some have assumed that the pore space in frozen soil is inherently a two-phase system, filled with only water and ice (no air) [e.g., *van Loon et al.*, 1991]. It is true that in an individual pore, ice and water can coexist only over a very narrow temperature range, at the lower limit of which the pore will spontaneously fill with ice. However, soils contain a range of pore sizes, and *Miller* [1973] predicted that in unsaturated soil, certain pores will fill with ice while others remain unfrozen, which was, by and large, confirmed by *Colbeck* [1982].

In the vicinity of a stationary ice front the soil may become saturated with time due to water migration from the unfrozen subsoil toward the freezing front. If the rate of water movement to the ice front cannot keep pace with the rate of energy loss to the soil surface, the freezing front will penetrate deeper, leaving an unsaturated profile with ice, water, and air present. In the 4 years (1989–1993) that we have been monitoring soil water distribution in an agricultural soil at the Rosemount Agricultural Experiment Station, Minnesota, only in 1 year was the profile near saturation prior to freezing. In the other years initial degree of saturation ranged from 0.25 to 0.75. In all years, a neutron moisture meter confirmed that most of the profile that was frozen remained unsaturated throughout the entire winter.

The amount of liquid water in a frozen soil is predominantly determined by the temperature. The  $\varepsilon$  value of the bulk soil at any given  $\theta_L$ , however, depends not only on the amount of liquid water but also on the amount of ice present, which in turn varies depending on the conditions prior to and during freezing. The volume fraction of ice equals the amount of water prior to freezing minus  $\theta_L$ , plus any water that migrated

to and froze at the point of interest. Consequently, we hypothesize that in frozen soil there is no unique relationship between bulk soil  $\varepsilon$  and  $\theta_L$ , but rather a family of calibration curves, each curve corresponding to a different total water content.

## Materials and Methods

### Gas Dilatometer

We chose to calibrate TDR with dilatometry, first introduced to soil science by *Bouyoucos* [1917], and since used by several scientists in different configurations [*Koopmans and Miller*, 1966; *Patterson and Smith*, 1981]. In these previous applications the apparatus consisted of a rigid, closed container filled with water-saturated soil. Soil water expands as it freezes, since ice is less dense than water; the resulting increase in the volume of the sample was monitored and used to calculate the amount of soil water that froze. The main disadvantage of this technique is that the soil needs to be completely saturated, which is usually accomplished by mixing water and soil to a paste, thus destroying the original soil structure.

We designed a new apparatus, which we call a gas dilatometer, that allows determination of  $\theta_L$  in frozen, intact soil samples at any degree of saturation. It is based on the same principle as the original dilatometer, namely, the expansion of water upon freezing. The difference is that the expansion of soil water in the gas dilatometer is measured by means of the increase in gas pressure surrounding the sample.

The gas dilatometer is a rigid container with a soil sample inside. Upon cooling, ice forms in the soil, and gas is displaced because ice is less dense than water. The result is a decrease in the total volume occupied by gas in the gas dilatometer, which consists of dead air space surrounding the sample and gas-filled pores in the soil sample. If the gas dilatometer is a closed system (hermetically sealed), gas pressure inside will increase during freezing, and decrease during thawing. Measurements of temperature and gas pressure in the gas dilatometer are sufficient to calculate changes in gas-filled volume using Boyle's law, from which the amount of water that has changed phase can be computed.

Our gas dilatometer is made of a copper core with a fixed bottom and a removable lid that contains an O-ring to hermetically seal the core (right-hand side of Figure 1). A temperature-controlled water bath (stability  $\pm 0.01^\circ\text{C}$ ; Neslab model RTE 110, Newington, New Hampshire) pumps a water-methanol mixture through copper tubing that is coiled around the outside over the entire length of the core. Heat-conductive putty fills the air space between the copper tubing and the core to optimize heat exchange between the core and the coil. Two eight-conductor, high-vacuum feedthroughs (Ceramaseal, New Lebanon, New York) welded in the lid provide electrical continuity through the lid yet maintain airtightness of the core. A precision, absolute pressure transducer (0.2-kPa accuracy, infinite resolution; Sensotec model TJE, Columbus, Ohio) measures gas pressure in the core. The core is insulated with spray foam and placed in a wooden box lined with Styrofoam; the remaining space in the wooden box is filled with Styrofoam chips. The pressure transducer is located outside the box and connected to the core by stainless steel tubing to thermally isolate the transducer from the core for optimum sensor stability. The box is then placed in a low-temperature growth chamber (Conviroon CMP 3244, Pembina, North Dakota), since even small temperature fluctuations in the laboratory affect temperature stability in the soil.

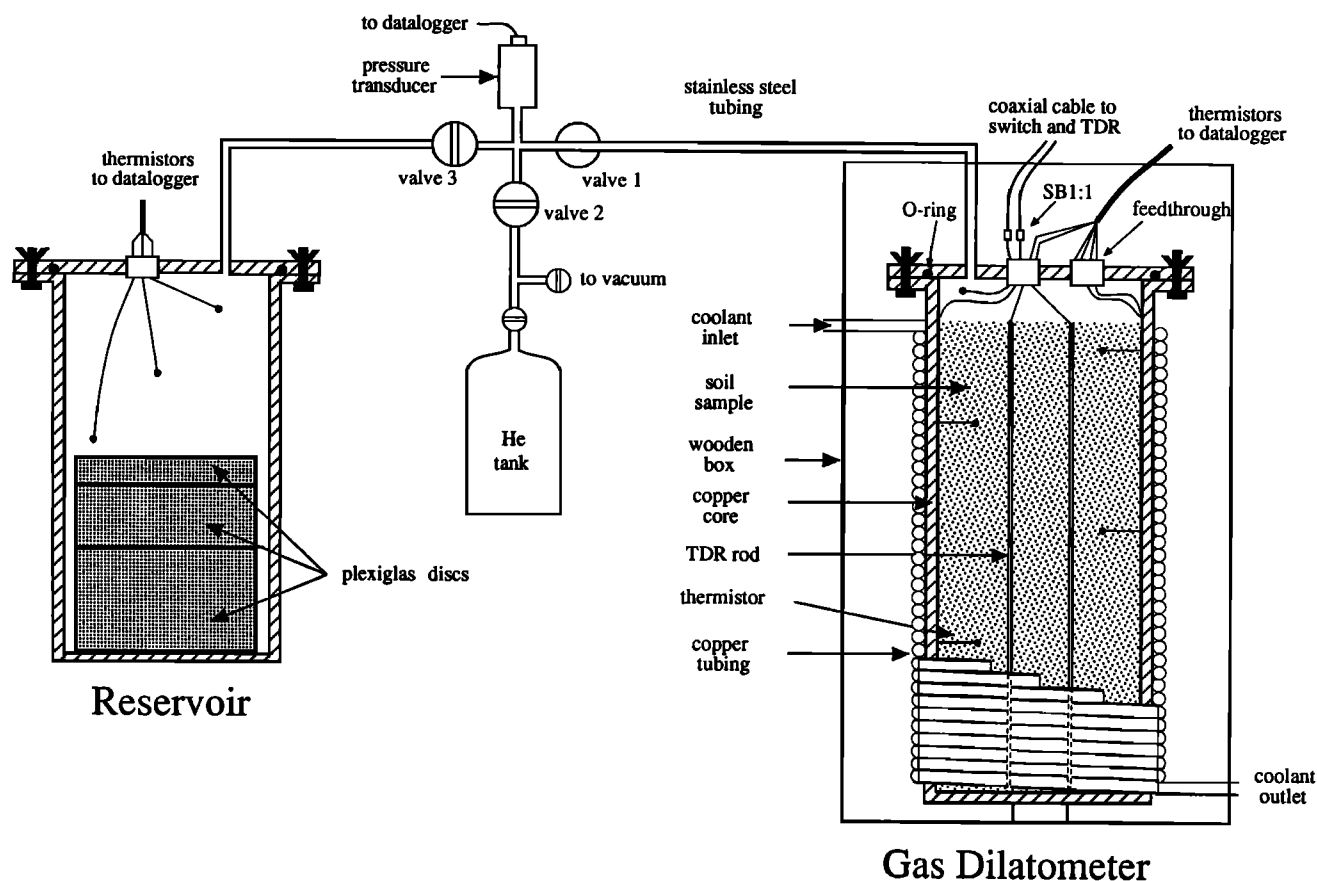


**Figure 1.** Apparatus to calibrate TDR for liquid water content in frozen soil. Gas dilatometer is shown on the right-hand side inside the wooden box. Constant-volume gas pycnometer consists of a reservoir (left-hand side) of known volume, connected to the gas dilatometer. The system is flushed by opening valve 2, pulling a vacuum, and then letting He into the system, after which valve 2 is closed again. During the actual TDR calibration, valve 1 is open, and valves 2 and 3 are closed, as shown. The reservoir is 23 cm high and 9 cm in diameter; the copper core is 32.8 cm high and 10 cm in diameter and rests on a polyvinyl chloride ring for better insulation. For clarity, not all lead wires from the feedthroughs are drawn, and only one pair of TDR rods is shown. Everything shown in Figure 1 is placed in a growth chamber at 2°C for optimal temperature stability and low thermal gradients between the gas dilatometer and its surroundings.

An intact soil sample (9.9-cm diameter, 33-cm length) was taken horizontally from the Ap horizon of a Waukegan silt loam (fine-silty over sandy or sandy-skeletal, mixed, mesic Typic Hapludoll). The slightly smaller diameter facilitated insertion of the large sample into the gas dilatometer and provided an additional path for gas exchange between soil air and dead air in the gas dilatometer. Five thermistors (YSI 44004, Yellow Springs, Ohio) were installed into the soil at depths of 4, 10, 16, 22, and 28 cm in a spiral fashion before the sample was inserted into the gas dilatometer, their leads extending along the side of the sample. A sixth thermistor was located in the space above the sample. Soil fragments from the upper surface of the sample were chipped away and removed with a vacuum cleaner to assure continuity of pores from the soil to the dead-air space, until the height of the sample was about 31 cm.

Soil moisture contents in the field were never small enough to allow taking a relatively dry, undisturbed sample. Therefore after the intact sample was removed from the gas dilatometer and oven-dried at the conclusion of the initial experiment, the same soil was rewetted with deionized water for a second run at a lower initial water content. To obtain a uniform bulk density, the sample was divided into 10 equal amounts, which

were subsequently inserted into the gas dilatometer. Each addition was packed so that it contributed 3 cm to the total depth; thermistors were placed 3, 9, 15, 21, and 27 cm from the bottom. The relatively dry, disturbed sample and the relatively wet, undisturbed sample will be referred to as the "dry sample" and the "wet sample," respectively.

Four stainless-steel rods (3.2-mm diameter, 0.3 m long) were inserted vertically into the soil in a square pattern, yielding two parallel pairs of TDR waveguides normal to each other, with a 3-cm spacing between the rods, allowing duplicate measurements of the soil  $\epsilon$ . Finally, vacuum grease was applied to the O-ring and the mating surfaces, lead wires from the thermistors and TDR rods were connected to the feedthroughs, and the lid was closed and bolted onto the flange of the copper core.

On the outside of the lid, the conductors from the feedthroughs leading to the TDR rods were connected to SB1:1 baluns [Spaans and Baker, 1993], which on the other side were connected to 50- $\Omega$  coaxial cable. These coaxial cables were connected to a TDR cable tester (Tektronix 1502B, Redmond, Oregon) through a two-position 50- $\Omega$  coaxial switch (JFW model 50S-597, Indianapolis, Indiana). This probe configuration closely simulates the probes we use in the field

(Midwest Special Services, St. Paul, Minnesota). The instrument settings of the TDR, data retrieval, and trace analysis were automated using a personal computer, which measured the apparent line length  $L_a$  (the distance between initial and final reflections on the TDR screen) from each probe every 10 min.

The thermistors were connected to a multiplexer (Campbell Scientific model AM416, Logan, Utah) and measured in a full bridge with lead wire compensation. All thermistors were individually calibrated against a secondary standard platinum resistance thermometer prior to installation. The thermistors and pressure transducer were monitored every 5 min using a data logger (Campbell Scientific, model CR7).

When temperature is changing in the gas dilatometer, gas-pressure equilibrium is a function of the heat conduction, the amount of phase change, and the gas permeability of the soil. The complex nature of the dynamics of these processes prohibits use of continuous freezing and thawing cycles, instead requiring stepwise changes in temperature with sufficient time for establishment of pressure and temperature equilibrium. To minimize the duration of the experiments and standardize equilibrium criteria, the data logger changed the bath temperature automatically to its next predetermined value when the pressure and temperature changed less than  $0.83 \text{ mPa s}^{-1}$  and  $1.67 \times 10^{-6} \text{ }^\circ\text{C s}^{-1}$ , respectively, over a 1-hour period.

The gas dilatometer must be a closed system, and all sinks and sources of gas inside must be eliminated or accounted for. Hermetically sealing the gas dilatometer is not a trivial requirement; the smallest leak will alter the pressure, creating a cumulative error that becomes significant considering the duration of the experiment (1–2 weeks). Microbial respiration was eliminated by incubating the soil with methyl bromide prior to the experiment. Interactions between gas and liquid are more complicated. When water freezes, gases are expelled from the crystalline structure of the ice and released into the gas phase; upon thawing, gases dissolve back into the liquid water. Temperature dependence of gas solubilities further complicates the matter. We decided to flush the gas dilatometer with He because it has a relatively low solubility in water that is nearly constant with temperature [Cady *et al.*, 1922]. In addition, the small molecular size of He speeds gas-pressure equilibrium inside the gas dilatometer and makes it less prone to entrapment by growing ice crystals that might block pores. Finally, He gas is inert and can be regarded as an ideal gas, obeying Boyle's law. In order to expel all other gases from the soil water, the soil was frozen and thawed twice, with the gas dilatometer flushed regularly with He during the process, so that eventually the only gases present in the gas dilatometer were He and water vapor. The amount of He in the liquid phase ( $n_L$ , in moles) can be calculated by

$$n_L = \alpha \frac{V_L P_{\text{He}}}{RT_0} \quad (2)$$

where  $R$  is the universal gas constant ( $8.314 \text{ J mol}^{-1} \text{ K}^{-1}$ ), and  $\alpha$  is the Ostwald absorption coefficient ( $9.37 \times 10^{-3}$  at  $2^\circ\text{C}$  [Cady *et al.*, 1922]), which is the volume of gas dissolved (reduced to 101.3 kPa and  $T_0 = 273.15 \text{ K}$ ) into a volume of liquid water ( $V_L$ , in cubic meters). Dorsey [1940, Table 234] concluded that  $n_L$  is linearly proportional to the partial He pressure ( $P_{\text{He}}$ , in pascals).

The mobility of He is a potential drawback; it leaks to the atmosphere more readily than other gases. We therefore chose an initial pressure such that the pressure inside the gas

dilatometer would remain below ambient pressure throughout the experiment. The large gradient in  $P_{\text{He}}$ , however, still favors He diffusion from the gas dilatometer toward the atmosphere, which can be minimized only with careful plumbing using He leak-tested valves, metal rather than plastic tubing, and welded connections wherever possible.

Conditions of high  $\theta_L$  and low  $\theta_i$  are established more easily by warming a frozen soil than by cooling an unfrozen soil, due to the nuisance of supercooling. Therefore the actual TDR calibration run started at  $-10^\circ\text{C}$  followed by one thawing and then one freezing cycle. Although the  $\theta_L(T)$  relation is hysteretic, the  $\varepsilon(\theta_L)$  relation is not, so it is immaterial whether the calibration is determined on a freezing or on a thawing cycle.

### Gas Picnometer

During freezing and thawing cycles changes in gas-filled volume inside the gas dilatometer ( $V_g$ ) were calculated from the pressure and temperature at equilibrium, and because the system is closed, one initial value for  $V_g$  suffices to calculate  $V_g$  at all subsequent equilibrium steps. We measured the initial value for  $V_g$  with a constant-volume gas picnometer [Torstenson and Erickson, 1936; Page, 1948; Danielson and Sutherland, 1986], which has the advantage of not disturbing the soil sample. This apparatus consists of a reservoir of known volume ( $V_g^*$ ) which is connected to the gas dilatometer (Figure 1). The reservoir and the gas dilatometer are initially at different pressures. Then they are connected and will assume the same pressure ( $P_{\text{II}} = P_{\text{II}}^*$ ), which will be somewhere between the values of the initial pressures. Hence  $V_g$  can be calculated with

$$V_g = V_g^* \left( \frac{P_{\text{II}}/T_{\text{II}}^* - P_{\text{I}}^*/T_{\text{I}}^*}{P_{\text{I}}/T_{\text{I}} - P_{\text{II}}/T_{\text{II}}} \right) - \frac{dn_L R}{P_{\text{I}}/T_{\text{I}} - P_{\text{II}}/T_{\text{II}}} \quad (3)$$

where  $P$  is air pressure (pascals),  $T$  is temperature (kelvins), subscripts I and II refer to measurements made before and after the reservoir and gas dilatometer are connected, variables with superscript asterisk are measured in the reservoir, and  $dn_L$ , which is the amount of He released from the water as  $P_{\text{He}}$  decreases, is calculated from (2). During the pycnometer experiment, valve 3 remains open (permitting flow). Values for  $P_{\text{I}}$  and  $T_{\text{I}}$  are measured with valve 1 open and valve 2 closed;  $P_{\text{I}}^*$  and  $T_{\text{I}}^*$  are measured after closing valve 1 and briefly opening valve 2 to lower the pressure in the reservoir. Finally, valve 1 is opened again to allow pressure equilibrium between the gas dilatometer and the reservoir, after which  $P_{\text{II}}$ ,  $T_{\text{II}}$ , and  $T_{\text{II}}^*$  are measured. Readings are always taken after pressure and temperature are stabilized.

The reservoir of the pycnometer was made of an aluminum core with a fixed bottom and a flange on top that supported a removable lid. The stainless steel lid contained an O-ring and a six-conductor high-vacuum feedthrough, allowing a temperature measurement using three thermistors inside the reservoir.

The highest resolution and lowest error for measuring  $V_g$  is obtained when its value is close to that of  $V_g^*$ , and when  $P_{\text{I}}$  and  $P_{\text{II}}$  are far apart. The first was realized by estimating  $V_g$  and placing Plexiglas discs of different thicknesses inside the reservoir to match  $V_g^*$  to  $V_g$  as closely as possible. The range of  $P$  is limited by the range of the transducer; values for  $P_{\text{I}}$ ,  $P_{\text{I}}^*$ , and  $P_{\text{II}}$  were of the order of 96, 10, and 50 kPa, respectively.

In summary, a soil sample within the gas dilatometer is instrumented with thermistors and TDR probes. The apparatus is incubated overnight with methyl bromide, subjected to two freeze and thaw cycles and frequent flushing with He to

expel all other gases from the system, and finally frozen to  $-10^{\circ}\text{C}$ . The gas dilatometer is then subjected to one stepwise thawing and freezing cycle, while  $P$ ,  $T$ , and  $L_a$  are continuously monitored. The last temperature on the thawing cycle is very close to but still below the melting point of the soil. The final temperature on the freezing cycle is  $-10^{\circ}\text{C}$ , so if the corresponding pressure is the same as the initial pressure, no leaks have occurred. The experiment is concluded by completely thawing the soil to obtain the final  $P$  and  $T$ , which are initial values for the calculation of  $\theta_L$ . Next,  $V_g$  is measured with the pycnometer following which the sample is removed from the gas dilatometer and its moisture content determined gravimetrically.

### Calculations

In addition to freezing or thawing of soil water, there are other temperature dependent variables that alter the pressure in the gas dilatometer from one temperature step to the next: (1)  $P_{\text{He}}$ , (2) the vapor pressure, and (3) the density of residual liquid water and ice (those fractions of water that are not involved in phase changes during that particular temperature step). In addition, the partitioning of He between gas and liquid phase (dissolved) depends on both  $\theta_L$  and on  $P_{\text{He}}$ .

The effect of temperature on  $P_{\text{He}}$  per se can be calculated with Boyle's law. Since the saturated vapor pressure  $e_s$  as a function of temperature is known, it can be subtracted from the measured gas pressure to yield  $P_{\text{He}}$ . A suitable approximation for  $e_s(T)$  for unfrozen conditions is [Campbell, 1977]

$$e_s = \exp \left( 52.57633 - \frac{6790.4985}{T} - 5.02808 \ln T \right) \quad (4)$$

where  $e_s$  is in kilopascals. An expression for  $e_s(\tau)$ , where  $\tau$  is temperature expressed in degrees Celsius, when ice was present was obtained by fitting a polynomial through tabular values [List, 1951] for the range  $-20^{\circ} < \tau < 0^{\circ}\text{C}$ :

$$e_s = 6.0986 \times 10^{-1} + 4.9333 \times 10^{-2}\tau + 1.6572 \times 10^{-3}\tau^2 + 2.2914 \times 10^{-5}\tau^3 \quad (5)$$

Hare and Sorensen [1987] developed a formulation for the density of liquid water ( $\rho_L$ ) as a function of temperature for  $-33^{\circ} < \tau < 10^{\circ}\text{C}$ :

$$\rho_L = \sum_{n=0}^6 a_n \tau^n \quad (6)$$

where  $a_0 = 999.86$ ,  $a_1 = 6.69 \times 10^{-2}$ ,  $a_2 = -8.486 \times 10^{-3}$ ,  $a_3 = 1.518 \times 10^{-4}$ ,  $a_4 = -6.9484 \times 10^{-6}$ ,  $a_5 = -3.6449 \times 10^{-7}$ , and  $a_6 = -7.497 \times 10^{-9}$ . The density of ice ( $\rho_i$ ) as a function of temperature was estimated by [Bader, 1964]

$$\rho_i = 9.1650 \times 10^2 - 1.4440 \times 10^{-1}\tau - 2.5470 \times 10^{-4}\tau^2 - 8.1147 \times 10^{-6}\tau^3 - 1.6295 \times 10^{-7}\tau^4 \quad (7)$$

For both (6) and (7),  $\rho$  is in kilograms per cubic meter. We assume that water and ice in soil have the same densities as in their respective bulk states. The thermal expansion of the soil minerals is neglected.

The amount of liquid water present after a step change in temperature can be calculated from the mass balance of the water ( $V_{L,j}\rho_{L,j} + V_{i,j}\rho_{i,j} = V_{L,j+1}\rho_{L,j+1} + V_{i,j+1}\rho_{i,j+1}$ ), Boyle's

law, (2), and conservation of the volume inside the gas dilatometer ( $V_{L,j} + V_{i,j} + V_{g,j} = V_{L,j+1} + V_{i,j+1} + V_{g,j+1}$ ):

$$V_{L,j+1} = \left[ V_{g,j} \left( \frac{P_{\text{He},j}}{P_{\text{He},j+1}} \frac{T_{j+1}}{T_j} - 1 \right) + V_{L,j} \left( \frac{\rho_{L,j}}{\rho_{L,j+1}} + \delta P_{\text{He},j} - 1 \right) + V_{i,j} \left( \frac{\rho_{i,j}}{\rho_{i,j+1}} - 1 \right) \right] \left( \frac{\rho_{L,j+1}}{\rho_{L,j+1}} + \delta P_{\text{He},j+1} - 1 \right)^{-1} \quad (8)$$

where

$$\delta = \frac{V_{g,j}}{n_j} \frac{P_{\text{He},j}}{P_{\text{He},j+1}} \frac{T_{j+1}}{T_j} \frac{\alpha}{RT_0}$$

$V$  is volume (cubic meters), subscripts i, L, and g refer to the ice, liquid, and gas phase, respectively, and subscripts  $j$  and  $j+1$  refer to subsequent temperature steps. If we define the initial state as the unfrozen state, then  $V_{i,j}$  is zero,  $V_{L,j}$  is measured gravimetrically,  $V_{g,j}$  is obtained from the gas pycnometer, and  $n_j$  is equal to  $P_{\text{He},j}V_{g,j}/RT_j$ . Dividing  $V_{L,j+1}$  by the volume of the soil sample yields  $\theta_{L,j+1}$ , the new liquid water content after the step change in temperature.

To evaluate the contribution from ice to the  $\epsilon$  of soil, the calibration of TDR in frozen soil was compared to a calibration in unfrozen soil. The same soil as from the frozen-soil calibration was moistened with deionized water and packed the same way as the "dry soil" sample to a bulk density of  $1.3 \text{ Mg m}^{-3}$ . A 0.3 m long, parallel probe with an SB1:1 balun in the head (Midwest Special Services) was inserted into the sample, and  $L_a$  was measured;  $\theta$  was determined gravimetrically.

## Results and Discussion

### Preliminary Experiments

After the gas dilatometer and the gas pycnometer were constructed, some preliminary experiments were conducted to test the performance of the setup and the calculations. Volumes of the reservoir and the gas dilatometer were determined from the difference between their weight when empty and when completely filled with water at a known temperature. This method of volume determination appeared more reproducible than calculating the volume from the dimensions, and it yielded  $1401 \text{ cm}^3$  for the reservoir and  $2569 \text{ cm}^3$  for the gas dilatometer at  $5^{\circ}\text{C}$ . A measurement with the pycnometer estimated the volume of the gas dilatometer to within  $5 \text{ cm}^3$  of its true value, demonstrating the high degree of accuracy that can be obtained by pycnometry. The rigidity of the gas dilatometer was tested by filling it with He only and subjecting it to a stepwise freezing and thawing cycle while measuring  $P$  and  $T$  at equilibrium. The calculated volume varied  $<0.06\%$  over the temperature range of  $-12^{\circ}$  to  $+5^{\circ}\text{C}$ , which is negligible.

If the sample in the gas dilatometer consisted of pure water only, then (8) should predict  $\theta_L = 1$  and  $\theta_i = 0$  above the freezing point, and  $\theta_L = 0$  and  $\theta_i = 1$  below it. We verified this by filling the gas dilatometer with distilled water and then freezing and thawing it three times while flushing it with He. Then the gas dilatometer was subjected to one freezing and thawing cycle, while  $P$  and  $T$  were measured. Equation (8) predicted  $\theta_L = 0.07$  below the freezing point. We attributed the overestimation of  $\theta_L$  to a lack of equilibrium between gaseous He and that dissolved in the water. Equilibration through still water is slow; Dorsey [1940, Table 236] reported a study where air concentration was measured in quiescent water that was initially air-free. After 100 hours the relative air con-

**Table 1.** Preliminary Experiment With 1259 g Distilled Water in the Gas Dilatometer

$P$ , kPa	$\tau$ , °C	$dPe$ , 10 <sup>2</sup> Pa	$dPT$ , 10 <sup>2</sup> Pa	$dPrW$ , 10 <sup>2</sup> Pa	$dPrI$ , 10 <sup>2</sup> Pa	$dPn$ , 10 <sup>2</sup> Pa	$dPpc$ , 10 <sup>2</sup> Pa	$\theta_L$ , m <sup>3</sup> m <sup>-3</sup>	$\theta_I$ , m <sup>3</sup> m <sup>-3</sup>	$\theta_g$ , m <sup>3</sup> m <sup>-3</sup>
89.008	4.14	...	...	...	...	...	...	1.000	0.000	0.000
87.630	0.31	-2.0	-12.2	0.1	0.0	0.0	0.3	0.996	0.004	-0.000
93.605	-5.51	-2.4	-18.5	-0.0	-0.0	0.0	80.7	-0.007	1.007	-0.083
92.573	-8.26	-0.8	-9.6	-0.0	-0.5	0.0	0.5	-0.013	1.013	-0.083
93.608	-5.50	0.8	9.6	0.0	0.5	0.0	-0.6	-0.007	1.007	-0.083
94.717	-2.62	1.1	10.0	0.0	0.5	0.0	-0.5	-0.002	1.002	-0.083
88.907	4.13	3.3	23.5	0.0	-0.0	0.0	-84.9	1.013	-0.014	0.001

Volume fractions of liquid water, ice, and gas are calculated with (8), assuming water is free of He throughout the experiment.

centration at 12-cm depth was only 75%. The depth of water in this experiment was 16 cm, and a relatively small area of water was exposed for only 1 day. Table 1 shows the calculations of  $\theta_L$  assuming that the water was free of He, which appeared a more realistic assumption when only pure water was involved. Estimation of the dead-air space above the water from the pycnometer improved also when water was assumed free of He. Similar results were obtained for a duplicate run. Approximate contributions to the total pressure changes from the changes in vapor pressure ( $dPe$ , from (4) or (5)), temperature ( $dPT$ , from Boyle's law), density of residual liquid water ( $dPrW$ , from (6)) and ice ( $dPrI$ , from (7)), He coming out of or going into solution ( $dPn$ , from (2)), and phase changes between liquid water and ice ( $dPpc$ ) are also shown in Table 1.

The water content in soil will be smaller than the amount of water used in these preliminary tests, so in soils,  $dPn$  will play a smaller role. Moreover, when unsaturated soil is in the gas dilatometer, the exposed surface to volume ratio of the soil water is very high, increasing the likelihood that gas phase and liquid phase He are in equilibrium. Dorsey [1940, Table 239] reported a study on the absorption of O<sub>2</sub> by a thin film of water that was initially free of O<sub>2</sub>. At a film thickness of 0.5 mm, the

relative O<sub>2</sub> concentration was 99% throughout after 40 s! Based on these considerations, we assumed that the water was always saturated with He when soil was involved. More details about the preliminary tests are given by Spaans [1994].

### TDR Calibration in Frozen Soil

An illustration of the time series of the three measured variables  $T$ ,  $P$ , and  $L_a$  from one temperature step to the next is shown in Figure 2. The graph shows how the pressure in the gas dilatometer rises first due to the temperature rise. As soil ice starts to melt (as indicated by the rise in  $L_a$ ), however, some air from the dead-air space will flow into the soil pores because water is denser than ice, thus reducing the overall pressure. The different dynamic responses of the variables confirm that only equilibrium data can be used for our purposes.

Results from the TDR calibration for  $\theta_L$  in the wet, frozen Waukegan silt loam are presented in Figure 3. The volume of the sample was 2390 cm<sup>3</sup>, with  $\rho_b = 1287$  kg m<sup>-3</sup>, and  $\theta = 0.355$ . The pycnometer test indicated  $V_g = 538$  cm<sup>3</sup>, of which roughly two thirds was soil air, and one third was dead-air space above the sample and in the tubing. The dead-air space should be kept as small as possible, since reducing  $V_g$  increases the sensitivity of the calculations (larger pressure change for

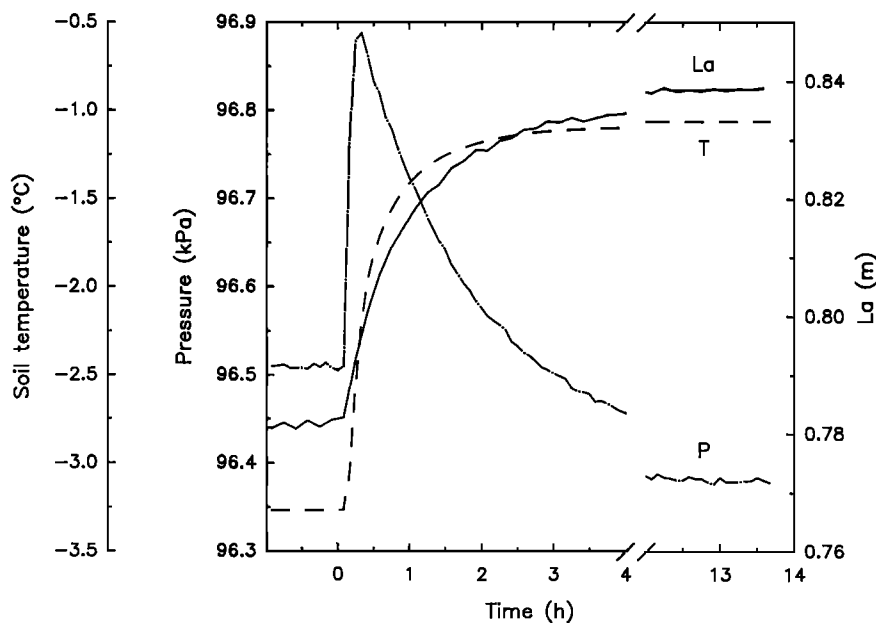


**Figure 2.** Responses of the soil temperature  $T$  (dashed curve), air pressure  $P$  (dot-dash curve), and apparent line length  $L_a$  (solid curve) after the temperature of the water bath is increased from  $-4^\circ$  to  $-1.3^\circ\text{C}$  at time 0. Equilibrium is reached 14 hours later.

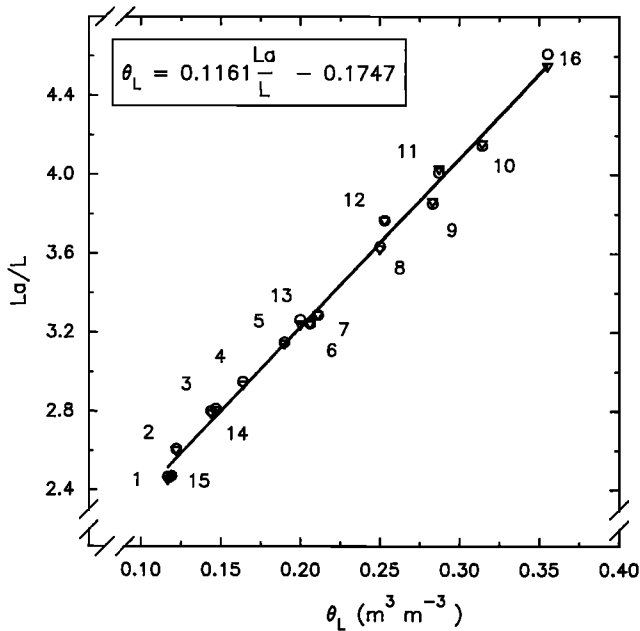


**Figure 3.** Ratio of apparent line length  $L_a$  to true line length  $L$  ( $= 0.3$  m) measured on two probes (circles and inverted triangles) with TDR as a function of liquid water content  $\theta_L$  in wet, frozen Waukegan silt loam. Numbers indicate the chronological order during calibration. All data points are in frozen soil except for point 16. Water content was independently measured only at point 16;  $\theta_L$  at all other points was calculated from (8). The equation shown in the inset is the best linear fit through all data, with a standard error of the estimate of  $\theta_L$  of  $5.9 \times 10^{-3}$  and  $R^2 = 0.994$ .

the same phase change). A small air space above the sample is required, however, to connect the thermistors and TDR rods to the feedthroughs before closing the lid.

Figure 3 shows that the data from the duplicate TDR probes agree closely, and they were all included in the linear regression. In practice, we measure  $L_a$  to find  $\theta_L$ , so  $\theta_L$  values were fitted as a function of  $L_a/L$ . The calibration was not extended beyond  $-10^\circ\text{C}$ , since soil temperatures at the site rarely drop

below that temperature. Moreover, most of the soil water is frozen at that temperature, so the contribution of phase changes to the total air pressure changes at lower temperatures becomes minor. Small uncertainties in the calculations and measurements will then cause relatively large errors in the estimation of  $\theta_L$ .

Table 2 illustrates the contributions of the different processes to the total pressure change for every temperature step, and shows that the model is most sensitive to changes in  $\theta_L$  at temperatures close to the melting point, where  $dP_{pc}$  is the major component of the pressure changes. Corrections for the changes in density of the residual water and ice appear to be of minor importance. The reproducibility of  $P$  at  $-10^\circ\text{C}$  indicates that leakage was negligible.

Temperature and pressure changes of the last freezing cycle prior to the experiment yielded  $\theta_L = 0.114$  at  $-10.40^\circ\text{C}$ , which is in excellent agreement with the value of 0.119 obtained during the final thawing cycle of the experiment. Another way to obtain  $\theta_L$  is to measure  $V_g$  in frozen and in unfrozen soil. The difference between these two values equals the mass of water frozen divided by  $\rho_i$  minus the mass of water frozen divided by  $\rho_L$ . Pycnometer experiments yielded  $V_g = 538$   $\text{cm}^3$  at  $1.15^\circ\text{C}$  and  $487$   $\text{cm}^3$  at  $-10.38^\circ\text{C}$ , from which  $\theta_L$  is calculated to be 0.116, a value consistent with the value obtained from the gas dilatometer experiment.

Results from the TDR calibration for  $\theta_L$  in the dry sample are shown in Figure 4. The dry sample was packed to a bulk density ( $1319$   $\text{kg m}^{-3}$ ) similar to that of the wet sample and moistened to  $\theta = 0.241$ . Measurements with the pycnometer yielded  $V_g = 794$   $\text{cm}^3$  in the unfrozen soil and  $763$   $\text{cm}^3$  at  $-10.5^\circ\text{C}$ , yielding  $\theta_L = 0.094$ , which is slightly lower than the 0.106 calculated from the dilatometer at the same temperature. Data from the two TDR probes agree closely, so they were both included in the regression. Contributions of the different processes to the total change in pressure for every temperature step are shown in Table 3. The pressure after the thawing and freezing cycle is within 50 Pa of the initial pressure, confirming that He leakage was again negligible. For both experiments, data obtained from freezing and thawing cycles are indistinguishable, confirming that there is no hysteresis in the  $\varepsilon(\theta_L)$  relationship.

**Table 2.** Volume Fractions of Liquid Water, Ice, and Air in Wet, Frozen Waukegan Silt Loam, Calculated From (8)

$P$ , kPa	$\tau$ , $^\circ\text{C}$	$dP_e$ , $10^2$ Pa	$dP_T$ , $10^2$ Pa	$dP_{rW}$ , $10^2$ Pa	$dP_{rI}$ , $10^2$ Pa	$dP_n$ , $10^2$ Pa	$dP_{pc}$ , $10^2$ Pa	$\theta_L$ , $\text{m}^3 \text{m}^{-3}$	$\theta_i$ , $\text{m}^3 \text{m}^{-3}$	$\theta_g$ , $\text{m}^3 \text{m}^{-3}$
88.295	1.15	...	...	...	...	...	...	0.355	0.000	0.152
93.869	-10.41	-4.1	-36.9	0.8	0.0	8.0	88.0	0.119	0.258	0.131
95.958	-1.75	2.8	30.9	-1.0	1.4	-1.3	-11.9	0.147	0.227	0.133
94.103	-0.36	0.6	4.9	-0.1	0.2	-2.1	-22.0	0.200	0.169	0.138
91.933	-0.12	0.1	0.8	-0.0	0.0	-1.9	-20.7	0.253	0.111	0.143
90.561	-0.08	0.0	0.1	-0.0	0.0	-1.2	-12.7	0.287	0.075	0.146
89.465	-0.05	0.0	0.1	-0.0	0.0	-0.9	-10.2	0.314	0.045	0.148
90.698	-0.08	-0.0	-0.1	0.0	-0.0	1.0	11.4	0.283	0.078	0.145
92.067	-0.11	-0.0	-0.1	0.0	-0.0	1.1	12.7	0.250	0.115	0.142
93.693	-0.22	-0.1	-0.4	0.0	-0.0	1.4	15.3	0.211	0.157	0.139
93.889	-0.24	-0.0	-0.1	0.0	-0.0	0.2	1.9	0.206	0.162	0.138
94.575	-0.34	-0.0	-0.3	0.0	-0.0	0.6	6.6	0.190	0.180	0.137
95.667	-0.56	-0.1	-0.8	0.0	-0.0	1.0	10.8	0.164	0.209	0.134
96.381	-1.06	-0.2	-1.7	0.0	-0.1	0.8	8.4	0.144	0.230	0.133
96.509	-3.27	-0.9	-7.8	0.1	-0.4	0.9	9.3	0.122	0.254	0.131
93.939	-10.38	-2.1	-25.3	0.8	-1.3	0.3	1.9	0.117	0.259	0.130

Unfrozen water content is measured gravimetrically at the end of the experiment; hence the data are shown in reverse chronological order. Duration of the experiment was 13 days.

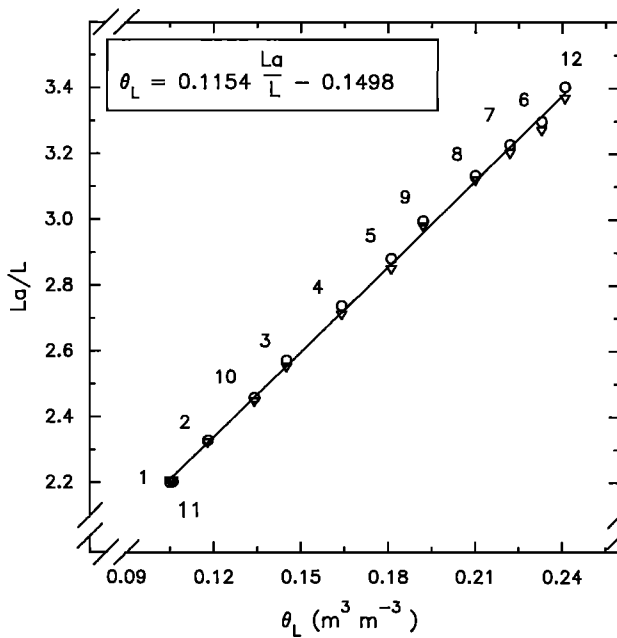


**Figure 4.** Ratio of apparent line length  $L_a$  to true line length  $L$  ( $= 0.3$  m) measured on two probes (circles and inverted triangles) with TDR as a function of liquid water content  $\theta_L$  in dry, frozen Waukegan silt loam. Numbers indicate the chronological order during calibration. All data points are in frozen soil except for point 12. Water content was independently measured only at point 12;  $\theta_L$  at all other points was calculated from (8). The equation shown in the inset is the best linear fit through all data, with a standard error of the estimate of  $\theta_L$  of  $2.1 \times 10^{-3}$ , and  $R^2 = 0.998$ .

If ice pressure and total solute content are invariable, a given frozen soil will have a reproducible  $\theta_L$  at any specific temperature, regardless of its total water content [Anderson and Morgenstern, 1973; Tice et al., 1982]. At essentially the same temperature ( $\approx -10.5^\circ\text{C}$ ) the wet sample, however, retained more liquid water ( $0.092 \text{ g g}^{-1}$ ) than the dry sample ( $0.080 \text{ g g}^{-1}$ ), but the difference is quite small and likely within experimental error.

#### Comparison to Other TDR Calibrations

Calibrations of TDR in frozen and unfrozen soil are compared in Figure 5. A best linear fit through data in unfrozen

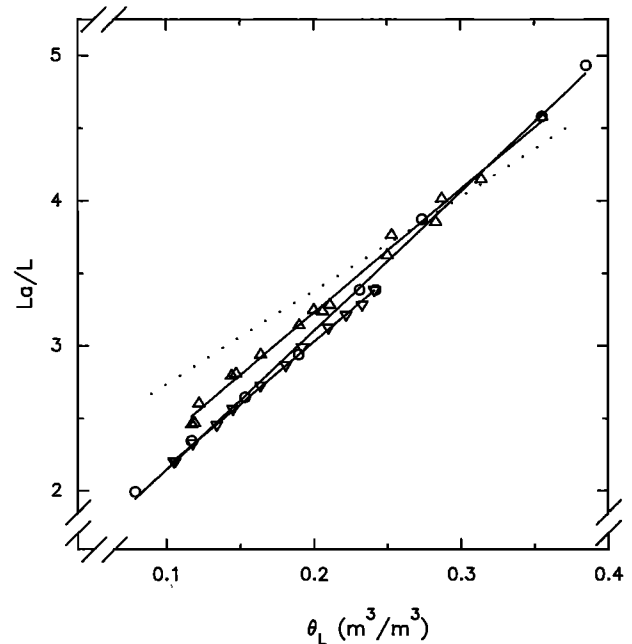


**Figure 5.** Comparison of different calibrations of TDR for liquid water content: relatively wet frozen Waukegan silt loam (triangles), relatively dry frozen Waukegan silt loam (inverted triangles), unfrozen Waukegan silt loam (circles), and Smith and Tice's [1988] equation (dotted line).

soil yielded  $\theta = 0.1039 L_a/L - 0.1225$ , with a standard error of the estimate of  $\theta$  of  $6.9 \times 10^{-3}$  and  $R^2 = 0.996$ . Consistent with our hypothesis, the slope  $d(L_a/L)/d\theta$  is significantly larger ( $P < 0.01$ ) in unfrozen than in frozen soil. In frozen soil the slopes of the calibration lines in the wet and dry samples are not significantly different ( $P < 0.01$ ). However, the intercept of the calibration line of the wet soil is significantly higher than that of the dry soil ( $P < 0.01$ ), which is explained by the contribution of ice. At identical  $\theta_L$  the wetter soil has consistently more ice than the drier soil, by an amount equal to  $(0.355 - 0.241)\rho_w/\rho_i = 0.124$ .

The  $\theta$  of the dry sample in unfrozen condition does not coincide with the calibration in unfrozen soil, but the difference in  $\theta$  is small (0.012) and probably within experimental error.

**Table 3.** Volume Fractions of Liquid Water, Ice, and Air in Dry, Frozen Waukegan Silt Loam, Calculated From (8)

$P$ , kPa	$\tau$ , $^\circ\text{C}$	$dPe$ , $10^2 \text{ Pa}$	$dPT$ , $10^2 \text{ Pa}$	$dPrW$ , $10^2 \text{ Pa}$	$dPrI$ , $10^2 \text{ Pa}$	$dPn$ , $10^2 \text{ Pa}$	$dPpc$ , $10^2 \text{ Pa}$	$\theta_L$ , $\text{m}^3 \text{ m}^{-3}$	$\theta_i$ , $\text{m}^3 \text{ m}^{-3}$	$\theta_g$ , $\text{m}^3 \text{ m}^{-3}$
94.933	0.96	...	...	...	...	...	...	0.241	0.000	0.250
94.327	-10.61	-4.1	-39.8	0.6	0.0	3.4	33.9	0.106	0.148	0.237
96.486	-2.89	2.3	27.7	-0.5	0.4	-0.8	-7.5	0.134	0.117	0.240
95.740	-0.57	1.0	8.2	-0.1	0.1	-1.5	-15.2	0.192	0.054	0.245
95.244	-0.48	0.0	0.3	-0.0	0.0	-0.5	-4.8	0.210	0.034	0.247
94.926	-0.42	0.0	0.2	-0.0	0.0	-0.3	-3.1	0.222	0.021	0.248
94.639	-0.41	0.0	0.0	-0.0	0.0	-0.3	-2.7	0.233	0.009	0.249
96.037	-0.59	-0.1	-0.6	0.0	-0.0	1.3	13.4	0.181	0.066	0.244
96.446	-0.79	-0.1	-0.7	0.0	-0.0	0.4	4.4	0.164	0.084	0.243
96.833	-1.22	-0.2	-1.5	0.0	-0.0	0.5	5.1	0.145	0.105	0.241
96.576	-3.84	-1.1	-9.3	0.1	-0.1	0.7	7.1	0.118	0.134	0.238
94.385	-10.53	-2.0	-23.9	0.4	-0.4	0.4	3.5	0.105	0.149	0.237

Sample volume was  $2360 \text{ cm}^3$ . Duration of the experiment was 4 days.

The calibration curve proposed by *Smith and Tice* [1988] underestimates  $\theta_L$  in frozen soil, even in the wet sample. In addition, it does not coincide with the calibration in unfrozen soil. One would expect that the two curves would converge, rather than diverge, at higher liquid water contents when the ice content approaches zero. *Smith and Tice* [1988], however, reported that their measurement system consistently yielded  $\epsilon \approx 72$  for bulk water instead of 80, which is curious in itself.

## Conclusions

We have shown that there is no unique calibration equation of TDR for liquid water content in frozen soil but that the calibration is dependent on the total water content. Two calibration equations to calculate  $\theta_L$  from  $L_a/L$  were obtained for Waukegan silt loam at total volumetric moisture contents of 0.36 and 0.24. The calibration lines have the same slopes but different intercepts because they have different ice contents at identical  $\theta_L$ . The slope  $d(L_a/L)/d\theta$  is larger for the calibration in unfrozen soil than in frozen soil because the difference between the permittivity of water and air is larger than that between water and ice.

To quantitatively understand the contribution of ice to the bulk soil  $\epsilon$ , more calibration curves at different initial water contents are required, which might lead to a more general calibration equation for TDR in frozen soil. The gas dilatometer provides a means to accomplish this task. However, the process requires considerable care and attention to detail for successful operation. Its design and construction turned out to be an enormous, time-consuming task, due mainly to inherent difficulty of creating an absolutely leak-free system. Once the system was operational, the calibration took 1 to 2 weeks, with little attention required since the entire system was automated. Good control of the temperature of both bath and environment is crucial; otherwise equilibration at temperatures very close to the melting point is virtually impossible.

The gas dilatometer is also an excellent tool to investigate interactions between water and ice potential, temperature, and pore saturation. Such knowledge should improve our understanding of water, energy, and solute flows in freezing and thawing soils.

## References

Anderson, D. M., and N. R. Morgenstern, Physics, chemistry, and mechanics of frozen ground: A review, in *Second International Conference on Permafrost*, pp. 257–288, Natl. Acad. of Sci., Washington, D. C., 1973.

Bader, H., Density of ice as a function of temperature and stress, *Spec. Rep.*, 64, 6 pp., U.S. Army Cold Reg. Res. and Eng. Lab., Hanover, N. H., 1964.

Baker, J. M., Measurement of soil water content, *Remote Sens. Rev.*, 5, 263–279, 1990.

Baker, J. M., and R. R. Allmaras, System for automating and multiplexing soil moisture measurement by time-domain reflectometry, *Soil Sci. Soc. Am. J.*, 54, 1–6, 1990.

Bouyoucos, G. J., Classification and measurement of the different forms of water in the soil by means of the dilatometer method, *Mich. Agric. Exp. Stat. Tech. Bull.*, 36, 48 pp., 1917.

Cady, H. P., H. M. Elsey, and E. V. Berger, The solubility of helium in water, *J. Am. Chem. Soc.*, 44, 1456–1461, 1922.

Campbell, G. S., *An Introduction to Environmental Biophysics*, 159 pp., Springer-Verlag, New York, 1977.

Colbeck, S. C., Configuration of ice in frozen media, *Soil Sci.*, 133, 116–123, 1982.

Danielson, R. E., and P. L. Sutherland, Porosity, in *Methods of Soil Analysis*, Part 1, *Agron. Monogr.* 9, 2nd ed., edited by A. Klute, pp. 443–461, Agron. Soc. of Am., Madison, Wis., 1986.

Dorsey, N. E., *Properties of Ordinary Water-Substance*, *Am. Chem. Soc. Monograph Ser.*, vol. 81, 673 pp., Reinhold, New York, 1940.

Gardner, W. H., Water content, in *Methods of Soil Analysis*, Part 1, *Agron. Monogr.* 9, 2nd ed., edited by A. Klute, pp. 493–544, Agron. Soc. of Am., Madison, Wis., 1986.

Goit, J. B., P. H. Groenevelt, B. D. Kay, and J. P. G. Loch, The applicability of dual gamma scanning to freezing soils and the problem of stratification, *Soil Sci. Soc. Am. J.*, 42, 858–863, 1978.

Hare, D. E., and C. M. Sorensen, The density of supercooled water, II, Bulk samples cooled to the homogeneous nucleation limit, *J. Chem. Phys.*, 87, 4840–4845, 1987.

Heimovaara, T. J., and W. Bouten, A computer-controlled 36-channel time domain reflectometry system for monitoring soil water contents, *Water Resour. Res.*, 26, 2311–2316, 1990.

Hoekstra, P., Moisture movement in soils under temperature gradients with the cold-side temperature below freezing, *Water Resour. Res.*, 2, 241–250, 1966.

Koopmans, R. W. R., and R. D. Miller, Soil freezing and soil water characteristic curves, *Soil Sci. Soc. Am. Proc.*, 30, 680–685, 1966.

List, R. J., *Smithsonian Meteorological Tables*, 6th ed., Smithsonian Inst., Washington, D. C., 1951.

Miller, R. D., Soil freezing in relation to pore water pressure and temperature, in *Second International Conference on Permafrost*, pp. 344–352, Natl. Acad. of Sci., Washington, D. C., 1973.

Nieber, J. L., J. M. Baker, and E. J. A. Spaans, Evaluation of soil water sensors in frozen soils, in *Road and Airport Pavement Response Monitoring Systems*, edited by V. C. Janoo and R. A. Eaton, pp. 168–181, Am. Soc. of Civ. Eng., New York, 1992.

Oliphant, J. L., A model for dielectric constants of frozen soils, in *Freezing and Thawing of Soil-Water Systems: A State of the Practice Report*, edited by D. W. Anderson and P. J. Williams, pp. 46–56, Am. Soc. of Civ. Eng., New York, NY, 1985.

Page, J. B., Advantages of the pressure pycnometer for measuring the pore space in soils, *Soil Sci. Soc. Am. Proc.*, 12, 81–84, 1948.

Patterson, D. E., and M. W. Smith, The measurement of unfrozen water content by time domain reflectometry: Results from laboratory tests, *Can. Geotech. J.*, 18, 131–144, 1981.

Smith, M. W., and A. R. Tice, Measurement of the unfrozen water content of soils; comparison of NMR and TDR methods, *Rep. 88-18*, U.S. Army Cold Reg. Res. and Eng. Lab., Hanover, N. H., 1988.

Spaans, E. J. A., The soil freezing characteristic: its measurement and similarity to the soil moisture characteristic, Ph.D. dissertation, 114 pp., Univ. of Minn., St. Paul, 1994.

Spaans, E. J. A., and J. M. Baker, Simple baluns in parallel probes for time domain reflectometry, *Soil Sci. Soc. Am. J.*, 57, 668–673, 1993.

Tice, A. R., J. L. Oliphant, Y. Nakano, and T. F. Jenkins, Relationship between the ice and unfrozen water phases in frozen soil as determined by pulsed nuclear magnetic resonance and physical desorption data, *Rep. 82-15*, U.S. Army Cold Reg. Res. and Eng. Lab., Hanover, N. H., 1982.

Torstenson, G., and S. Erickson, A new method for determining the porosity of the soil, *Soil Sci.*, 42, 405–417, 1936.

van Loon, W. K. P., E. Perfect, P. H. Groenevelt, and B. D. Kay, Application of dispersion theory to time domain reflectometry in soils, *Transp. Porous Media*, 6, 391–406, 1991.

J. M. Baker, and E. J. A. Spaans, Department of Soil, Water, and Climate, University of Minnesota, 1991 Upper Buford Circle, St. Paul, MN 55108. (e-mail: espaans@soils.umn.edu)

(Received February 13, 1995; revised July 31, 1995; accepted August 31, 1995.)